Heliyon 11 (2025) e41691

Contents lists available at ScienceDirect

Heliyon

journal homepage: www.cell.com/heliyon

Research article

Influence of environmental variables and anthropogenic activities on soda-saline lakes chemistry in northern Tanzania: A remote sensing and GIS approach

Azaria Stephano Lameck [a,b,*], Brian Rotich [a,f], Abdalrahman Ahmed [c,d], Harison K. Kipkulei [g,h,i], Peto Akos [a], Emil Boros [e]

[a] Doctoral School of Environmental Science, The Hungarian University of Agriculture and Life Sciences, Pa´ter Ka´roly u. 1, Go¨d¨oll¨o, 2100, Hungary
[b] Department of Earth Science, Mbeya University of Science and Technology, PO BOX 131, Mbeya, Tanzania
[c] Institute of Geomatics and Civil Engineering, Faculty of Forestry University of Sopron, Bajcsy-Zsilinszky ut. 4, Sopron, 9400, Hungary
[d] Department of Forest and Environment, Faculty of Forest Science and Technology, University of Gezira Wad Madani, Sudan
[e] Institute of Aquatic Ecology, Centre for Ecological Research, Karolina str. 29. Budapest, 1113, Hungary
[f] Faculty of Environmental Studies and Resources Development, Chuka University, P.O. Box 109, 60400, Chuka, Kenya
[g] Humboldt Universita¨t zu Berlin, Faculty of Life Sciences, Invalidenstrafie 42, 10115, Berlin, Germany
[h] Department of Geomatic Engineering and Geospatial Information Systems, Jomo Kenyatta University of Agriculture and Technology, P.O. Box, 62000, Nairobi, 00200, Kenya
[i] University of Augsburg, Faculty of Applied Computer Sciences, Institute of Geography, Alter Postweg 118, 86159, Augsburg, Germany

ARTICLE INFO

Keywords:
Soda-saline lakes
Climate variability
Soil type
Geology
Land use /land cover change

ABSTRACT

This study employed Remote Sensing and Geographical Information Systems to explore the influence of environmental factors and human-induced land use/land cover changes on the chemistry of soda-saline lakes in Northern Tanzania. Satellite-based rainfall data were sourced from the Climate Hazards Group Infrared Precipitation with Station (CHIRPS) datasets, and temperature data were obtained from MERRA-2. Monthly precipitation, temperature, and drought conditions in lake watersheds were analyzed from 1981 to 2022, while land use and land cover changes were assessed for 2000, 2014, and 2023. Soil types were acquired from the FAO Digital Soil Map of the World, while geological characteristics were sourced from the US Geological Survey database. The findings revealed that the region's climate is ideal for enhancing evapotranspiration, leading to mineral precipitation, and altering the chemistry of soda-saline lakes. The Standardized Precipitation Evapotranspiration Index revealed increased drought events in the lake basins since 1987, with prolonged drought occurrence between 2000 and 2017. The results also showed that the region is characterized by a variety of soil types, including ferric acrisols, chromic cambisols, calcic cambisols, entisols, inceptisols, eutric fluvisols, distric nitisols, humic nitisols, mollic andosols, ochric andosols, and pellic vertisols. Furthermore, the region is distinguished by diverse geological processes, from Precambrian-Cambrian to tertiary intrusive, triggered by volcanic and tectonic activity. Land use/land cover changes results indicated dynamics in the various classes with an overall decrease in areas under water bodies (—39.80 %), forests (—22.57 %) and bareland (—36.18) while agricultural land (111.01 %) built-up areas (434.72 %), shrubs and grasses (72.77 %) increased in area coverage over the 23 years study

* Corresponding author. Doctoral School of Environmental Science, The Hungarian University of Agriculture and Life Sciences, P´ater Ka´roly u. 1, Go¨do¨llo¨ 2100, Hungary.
E-mail addresses: azariastephano@gmail.com, Lameck.Azaria.Stephano@phd.un-mate.hu (A.S. Lameck).
Other emails: brotich@chuka.ac.ke

https://doi.org/10.1016/j.heliyon.2025.e41691
Received 10 July 2024; Received in revised form 26 December 2024; Accepted 2 January 2025
Available online 3 January 2025

period (2000–2023). This study underscores the complex interplay between environmental variables and human activities in shaping the chemistry of soda-saline lakes.

1. Introduction

Soda and soda-saline lakes are two distinctive types of inland saline waters characterized by high pH (pH > 9) and high alkalinity. However, they differ in the relative proportions of dissolved ions [1]. Soda lakes have Na^+ > 25 % and are first in the cation dominance sequence, whereas $HCO_3^- + CO_3^{2-}$ > 25 e%, ranked first in the anion dominance sequence [1]. In contrast, soda-saline lakes Na^+ > 25 e % and ranked first in the cation dominance sequence, and $HCO_3^- + CO_3^{2-}$ > 25 e% but not ranked second after Cl^- or SO_4^{2-} e% [1]. Both soda and soda saline lakes are characterized by lower dissolved alkaline earth metal ions (Ca^{2+} and Mg^{2+}) [1]. Soda and soda-saline lakes are vital biodiversity hotspots, supporting microbial life like cyanobacteria, haloarchaea, and algae [2–4] while providing crucial habitats for waterbirds, particularly flamingos and some fish species [5,7]. They are highly productive due to abundant photosynthetic microorganisms [2–4] and serve as important CO_2 sinks. These lakes also help filter water and cycle essential nutrients like nitrogen, Sulphur, carbon, and phosphorus [8–10], supporting and maintaining the health of these ecosystems. Economically, they are valuable for industries such as soda ash production, fishing, aquaculture, biotechnology, and ecotourism [11–14].

The chemical composition of soda-saline lakes is shaped by interactions between the lake water and its surrounding environment [15], including climate dynamics, soil mineralogy, geological processes, and human activities [16]. Climate variations, such as changes in rainfall and evaporation, directly influence lake salinity and water chemistry [17]. Droughts trigger acidification, brownification, raise salinity, alter pH, and disrupt the balance of these ecosystems [18–22]. The mineral composition of surrounding soils is crucial for the lake's alkalinity, with sodic soils contributing Na^+ and CO_3^{2-} ions through weathering and erosion [19,23,24]. Sodic soils, which are alkaline and rich in Na^+ and CO_3^{2-}, affect soda-saline lake's chemical properties [24,25]. The geological formations beneath lake basins play a key role in influencing lake water chemistry, which can vary based on the area's geological characteristics [26–28]. Volcanic or tectonic activity introduces unique chemical features to the lake [18,29,30]. Weathered volcanic rocks like basaltic, trachytic, and carbonatite ashes release CO_3^{2-} and HCO_3^-, increasing lake alkalinity [19,31,32]. Soluble carbonate minerals, including nahcolite ($NaHCO_3$), trona ($Na_3H(CO_3)_2{\cdot}2H_2O$), thermonatrite ($Na_2CO_3{\cdot}H_2O$), pirssonite ($CaCO_3{\cdot}Na_2CO_3{\cdot}2H_2O$), gaylussite ($CaCO_3{\cdot}Na_2CO_3{\cdot}5H_2O$), and calcite ($CaCO_3$), further alter the lake's chemical compositions [33]. Additionally, inflow waters in volcanic regions also gain alkalinity from the hydrolysis of volcanic sediments [34,35]. Human activities, such as agriculture and urbanization, impact lakes by increasing nutrient runoff, salinity, and sedimentation, disrupting their ecological balance [17,37]. Agricultural operations runoffs introduce fertilizers and pesticide residues into the lakes, altering chemistry and nutrient levels and promoting harmful algal blooms [36]. Urban development increases impervious surfaces, altering runoff patterns and increasing sedimentation [38,39]. Deforestation exacerbates these effects by increasing erosion, which leads to higher sediment and nutrient loads in the lakes [39]. Clearing vegetation exposes soils and rocks to weathering and erosive processes, resulting in increasing sediment loads and nutrient inputs into lake waters [40].

The northern region of Tanzania, particularly the Eastern arm of the East African Rift Valley (EARV), is home to many soda-saline lakes [13,41]. Previous studies have focused on the physical and chemical properties of these lakes [5,6,13,33,35,42–46]. Other research in the region has focused on climatic conditions and geological aspects [12,47–52] but have not fully explored their interactions and influence on lake chemistry. The limited understanding of how environmental factors and human activities affect their chemistry is the motive behind this study. This study examines how environmental factors and human activities impact the chemistry of soda-saline lakes in Northern Tanzania by employing remote sensing (RS) and geographical information systems (GIS). The integration of these technologies provides valuable insights into the region's climate, soil composition, geology, and land use/land cover (LULC) changes. Understanding the impact of these environmental drivers and anthropogenic changes is critical for maintaining the chemical balance and ecological health of these ecosystems.

2. Material and methods

2.1. Description of the study area

This study covers environmental variables (climate, soils, geology, land use, and land cover change) around Northern Tanzania's three soda-saline lakes (Natron, Manyara, and Eyasi). Lake Natron and Manyara are soda lakes, whereas Lake Eyasi is a soda-saline, as highlighted in Table 1 [13].

Table 1
The dominance trend of the ionic concentrations of Lake Eyasi, Natron and Manyara [13].

Lakes	Dominant ions sequence		Water chemical types
	Cations	Anions	
Eyasi	$Na^+ > K^+ \sim Mg^{2+} \sim Ca^{2+}$	$Cl^- > HCO_3^- + CO_3^{2-} > SO_4^{2-}$	Soda-saline
Natron	$Na^+ > K^+ > Mg^{2+} \sim Ca^{2+}$	$HCO_3^- + CO_3^{2-} > Cl^- > SO_4^{2-}$	Soda
Manyara	$Na^+ > K^+ \sim Mg^{2+} \sim Ca^{2+}$	$HCO_3^- + CO_3^{2-} > Cl^- > SO_4^{2-}$	Soda

Geographically, the study area is located between 4°30′- 1°30′S latitude and 34°0′- 38°0′E longitude. The lakes are bordered by the Ngorongoro, Longido, Monduli, Karatu, Meatu, and Babati districts (Fig. 1(a–c)). The area is characterized by an arid and semi-arid climate, where temperatures typically drop to around 2 °C during June or July and commonly reach highs of 35 °C in February, September, and October [52,53]. The area has two distinct seasons: the rainy season starts in late October and ends in early May, and the dry season begins in June and lasts until early October. In the arid lowland plains, the rainfall ranges from 400 to 600 mm/year, whereas in the mountainous forested areas, the rainfall ranges from 1000 to 1200 mm/year [54]. The area is covered with a diverse array of vegetation, ranging from short grasslands and shrubs in the lowland plains to dense forests in the mountainous areas [53]. This diverse plant life creates homes for a wide range of wildlife and rare bird species. The region's distinct climate and wildlife make it an ideal place for ecotourism and wildlife conservation activities, bringing tourists worldwide to enjoy its natural beauty and biodiversity. The geological features of the area are influenced by active volcanic activity and tectonic movements, which are the ongoing processes within the East African Rift Valley [12,55]. The volcanism and tectonic movements are responsible for the formation of landscapes in the area. The local community in the area are mainly involved in farming and livestock rearing. They commonly grow crops like maize, beans, and vegetables. Livestock such as cattle, goats, and sheep are also raised for meat and dairy production, making a substantial contribution to the local economy and the livelihoods of residents.

2.2. Data acquisition, classification and analysis

2.2.1. Temperature and precipitatation

This study used satellite-based rainfall and temperature data collected from predetermined locations within the catchment area of each lake. Satellite-based climatic data over historical data from the catchment area meteorological station was used due to data limitations and unequal geographical coverage [52]. However, the satellite-based climate data underwent quality control and was validated using weather station data from the Arusha Meteorological Authority. The satellite-based rainfall data were sourced from the Climate Hazards Group Infrared Precipitation with Station (CHIRPS) datasets [56]. The CHIRPS is a product of the collaborative effort between the United States Geological Survey (USGS) and the University of California Santa Barbara (UCSB). It provides rainfall data with a spatial resolution of 0.05° [56] and daily temporal resolution. The satellite-derived temperature data was obtained from MERRA-2, a component of the National Aeronautics and Space Administration of Worldwide Energy Resource (NASA POWER) project. We acquired daily precipitation data from CHIRPS and maximum and minimum temperature data through MERRA-2 from NASA POWER [57] for the period spanning from 1981 to 2022. MERRA-2 from the NASA POWER project provides the maximum and minimum temperature with a spatial resolution of 0.5° [57]. The processing workflows for CHIRPS/MERRA-2 data and station data are detailed in Fig. 2 (a and b).

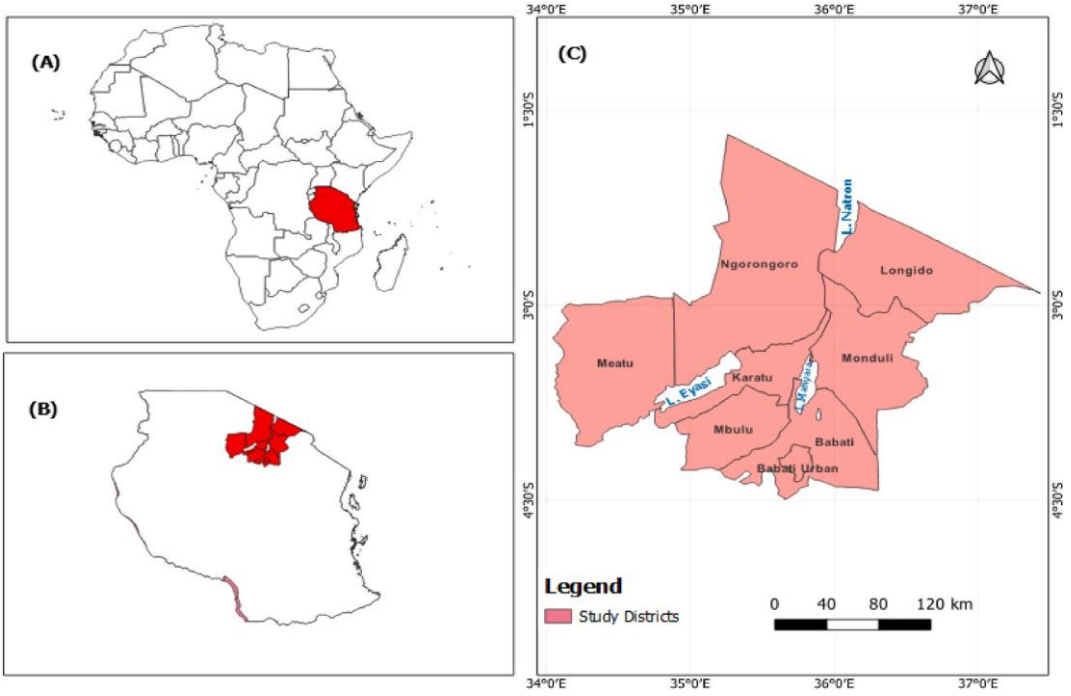

Fig. 1. The map of the study area (A) depicts the location of Tanzania in Africa (B) Location of the study area in Tanzania (C) Location of the three soda saline lakes in Northern Tanzania.

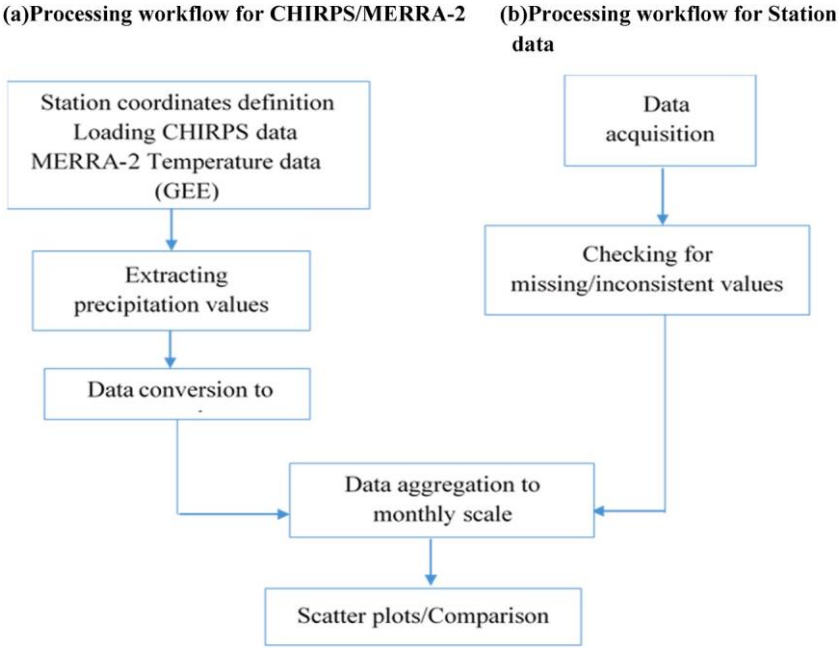

Fig. 2. Processing workflow for (a) Processing workflow for CHIRPS/MERRA-2 and (b) Processing workflow for Station data.

2.2.2. Drought analysis

The satellite-based climate data were also used to assess and monitor drought incidence in the studied area basins from 1982 to 2022. The Standardized Precipitation Evaporation Index (SPEI), developed by Ref. [58], was applied to assess drought conditions within the studied basins. The index is an improvement of the original Standardized Precipitation Index (SPI), both used to quantify and monitor drought circumstances in any part of the globe. SPEI includes both temperature and rainfall as inputs in its calculation, which is different from the initial SPI, which only utilized precipitation. The SPEI index determines the difference between potential evapotranspiration (PET) and rainfall to establish the water balance at any given location. PET is usually computed using the Penman-Monteith, Thornthwaite (TW), or Hargreaves (HG) techniques, with the methods differing on the variables used to determine the PET. The index can be calculated at different time scales, with the typical timescales being 3 months, 6 months and 12 months. These scales are ideal for examining the short, medium, and long-term drought conditions. The SPEI computation was calibrated in the study using observed climatic data at the different lake basins. The calibration involved a linear bias-correction scaling applied to match the monthly mean values of the corrected precipitation (Eq (1)) and temperature (Eq (2)) variables with the observed values. Precipitation was corrected with a multiplier and temperature with an additive term on a monthly scale. The correction and the SPEI computation were implemented in R using the SPEI, zoo and its packages.

$$\text{Preccal} = \text{Precraw} * \mu(\text{Precobs})/(\mu(\text{Precraw}) \quad (1)$$

$$\text{Tcal} = \text{Traw} + \mu(\text{Tobs}) - \mu(\text{Traw}) \quad (2)$$

The calibration process is crucial to avoid biased interpretations and several other problems, such as the false severity of environmental conditions. The monthly observed rainfall and temperature data from 1981 to 2022 used for calibrating the climatic variables were obtained from the Tanzania Meteorological Authority (TMA).

2.2.3. Water quality assessment

Various spectral indices were utilized to assess the water quality of the three lakes on Google Earth Engine (GEE). The indices comprised the Normalized Difference Water Index (NDWI), and the Chlorophyll Index (CI), derived from Landsat 7 and Landsat 8 satellite imagery for the years 2000, 2014, and 2023. NDWI is useful for assessing water presence, surface wetness, and water quality [59]. The NDWI values typically range from —1, indicating low moisture, absence of water or high turbidity levels, to +1 indicating high moisture or the presence of open water [60,61]. The Chlorophyll Index (CI) on the other hand measures the concentration of chlorophyll, which is a proxy for algal growth and overall productivity in water bodies. Higher CI values indicate higher chlorophyll concentrations, suggesting increased algal biomass, which may be associated with eutrophication or changes in nutrient levels [62].

The respective indices were calculated using equations (3) and (4).

$$NDWI = \frac{\text{Green} - \text{Nir}}{Green + Nir} \quad (3)$$

Where:

$NDWI$ = Normalized Difference Water Index,
$Green$ ¼ reflectance in the green band,
NIR = reflectance in the near-infrared band.

$$CI = \frac{\rho_{NIR}}{\rho_{green}} - 1 \quad (4)$$

where:

CI = Chlorophyll Index,
ρNIR = reflectance in the near-infrared (NIR) band,
$\rho Green$ = reflectance in the green band.

2.2.4. GIS-based soil types classification

In this study, we retrieved the soil information from the FAO Digital Soil Map of the World (DSMW). The FAO Digital Soil Map of the World (DSMW) is a digital version of the FAO-UNESCO Soil Map of the World, prepared on paper at a scale of 1:5 million [63]. The DSMW provides detailed information on various soil classes and properties, such as texture, pH levels, and organic matter content [63]. The DSMW shapefile was downloaded and imported using the "add layer" function into the QGIS software (QGIS version 3.22.10). The imported shapefile was clipped using the "clip" tool in QGIS based on the study area shapefile. This ensured that only the relevant soil information within the study area was retained for further analysis. The clipped soil map was then categorized into different soil classes based on the FAO-UNESCO Legend, allowing for a more in-depth understanding of the soil composition within the study area. We employed this comprehensive dataset to examine the spatial distribution of various soil types across the study area and evaluate their correlations between specific soil types and the chemistry of the soda-saline lakes.

2.2.5. GIS-based geological features classification

The underlying geological information for the study area was derived from world geological maps from the USGS database. We downloaded the world geological map files from the USGS database in QGIS-compatible formats. Using the "add layer" function within QGIS, the downloaded geological map was imported into the QGIS project. To assure accuracy, the datasets underwent extensive data cleaning, which included converting all files to a common Coordinate Reference System (CRS). Subsequently, the world geological map file sourced from the USGS was merged with the study area shapefile through the "clip" function. Following the completion of the integration process, a comprehensive classification of the geological features present in the study area was conducted. Each geological unit was accurately categorized, with distinct colours, patterns, and symbols assigned to facilitate clear differentiation on the map.

2.2.6. Land use land cover (LULC) changes

2.2.6.1. Remote sensing dataset and processing. Landsat satellite images from 2000, 2014, and 2023 were used to analyze LULC changes in Northern Tanzania over the 23-year study period. These specific years were chosen to identify changes over both the short and long terms, while also considering the availability of cloud-free images with less than 5 % cloud cover. We utilized images from the Landsat-5 Thematic Mapper (TM) and the Landsat-8 Operational Land Imagery (OLI) archives available on the Google Earth Engine (GEE) platform. The images were processed on the GEE platform to classify LULC types within the study area. GEE provides a vast archive of geospatial data, including satellite imagery, which facilitates large-scale analysis. We processed spectral bands (Blue, Red, Near Infrared, and Shortwave Infrared) and derived indices such as the Normalized Difference Vegetation Index (NDVI), Normalized Difference Built-up Index (NDBI), and Normalized Difference Moisture Index (NDMI). These spectral bands and indices were then used as input features for the supervised classification process. The bands had a spatial resolution of 30 m. Satellite images were acquired from within the same season for each year to ensure consistency and minimize the effects of moisture and phenological differences [64]. We selected images captured from June to September, corresponding to the driest period in the study area, to reduce cloud cover and ensure comprehensive coverage and consistency.

2.2.6.2. Image processing and classification. The Landsat images were processed in GEE and then exported to QGIS version 3.28.6 for classification and the creation of final LULC change maps. Six LULC classes were identified including water bodies, forests, shrubs/grasses, bareland, agricultural land, and built-up areas. For each image classification, a minimum of 330 samples were selected by drawing polygons. These samples were randomly divided into two equal groups, with 50 % used for training and 50 % for validating the classification accuracy [65]. Additionally, visualization was enhanced by using different-colour composites of the satellite images. Supervised classification was conducted using the Dzetsaka plugin in QGIS, which supports various machine-learning algorithms. Additional dependencies were installed to utilize Dzetsaka's algorithms, including the Scikit-learn 1.0.1 Python package, a standard library for machine learning [66,67]. The Random Forest (RF) classifier was employed to classify the three Landsat images due to its robustness in distinguishing various LULC classes across different environment areas [68,69] as well as its high accuracy in the study. The RF algorithm was trained using reference data gathered through a combination of fieldwork, existing base maps (topographical maps), and feature digitization from Google Earth using interpretation elements such as size, texture, tone, and shapes. The accuracy assessment of the study area was based on the confusion (error) matrix derived from the classified LULC data. The LULC classification is considered incomplete until the accuracy meets the satisfactory threshold defined by Ref. [70] criteria. This analysis employed Kappa

statistics and overall accuracy to evaluate the classification results.

3. Results and discussion

3.1. Validation of CHIRPS and MERRA-2 data

Fig. 3 (a, b) presents the validation results for CHIRPS (precipitation) data and MERRA-2 (temperature) data against the station data. The results showed an RMSE of 0.94 ($R^2 = 0.54$) for the station-recorded temperature data and MERRA-2 temperature data, and an RMSE of 65.52 ($R^2 = 0.53$) for station-observed precipitation and CHIRPS data. The results suggest that the satellite-based MERRA-2 temperature data and CHIRPS precipitation data retrieved from the established stations are reliable and suitable for use in drought-related studies.

3.2. Climate variability

The satellite-based data on rainfall and temperature from 1981 to 2022 in the catchments of the three soda-saline lakes (Manyara, Natron, and Eyasi) in Northern Tanzania is shown in Fig. 4 (a–f). The results revealed similar precipitation and temperature distribution patterns across the catchment areas of Lake Manyara, Natron, and Eyasi, with only minor differences seen amongst the lakes. The rainfall data revealed that the region experiences precipitation between late October and May. However, the maximum rainfall peak occurs in the fall (March–May), while the minimum rainfall occurs in November, December, January, and February. These observed precipitation distribution patterns are similar to those reported in earlier studies conducted in the region [52,71]. This pattern suggests a distinct wet season in Northern Tanzania during these months. Precipitation enhances the weathering process of the adjacent rocks and minerals, causing the chemical constituents to enter the lakes. This influx of chemical constituents from the surrounding soils influences the chemical compositions of the soda-saline lakes. On the other hand, the temperature data shows that the region consistently experiences maximum temperatures between 25 and 35 °C throughout the year, with the peak months being January, February, March, September, and October. In contrast, the minimum temperature ranges from 6 to 17 °C in June and July. The observed temperature distribution patterns in the catchment areas of soda-saline lakes in northern Tanzania exhibit similarities to the findings previously reported by Ref. [52]. In this semi-arid climate, a higher temperature induces larger evaporations, which usually exceed precipitation levels, altering the chemical dynamics of the soda-saline lakes. Higher temperatures observed in the region allow evaporation, concentrating salts and minerals in the water and giving soda-saline lakes their characteristic high salinity levels. This pattern of temperature and evaporation in the area plays a crucial role in shaping the ecosystem and biodiversity of the soda-saline lake. Overall, the satellite data provides valuable insight into the seasonal variations in rainfall and temperature within the catchments of the soda-saline lakes in Northern Tanzania.

3.3. Drought analysis

Fig. 5 shows the time series of the SPEI at 3-month, 6-month, and 12-month timescales calculated using a 40-year-long series of rainfall and temperature data in three lake basins in northern Tanzania. The SPEI was used to establish the spatio-temporal trends of droughts in the study area. Consequently, we modelled 3-month, 6-month, and 12-month SPEI for the various lake basins

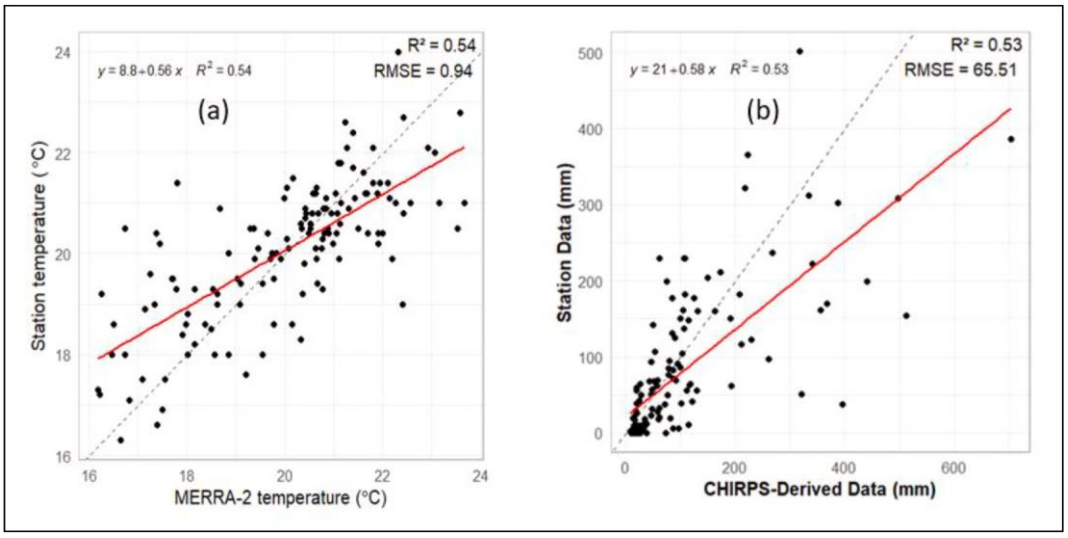

Fig. 3. (a) Station temperature versus MERRA-2 temperature data (b) observed precipitation versus CHIRPS data.

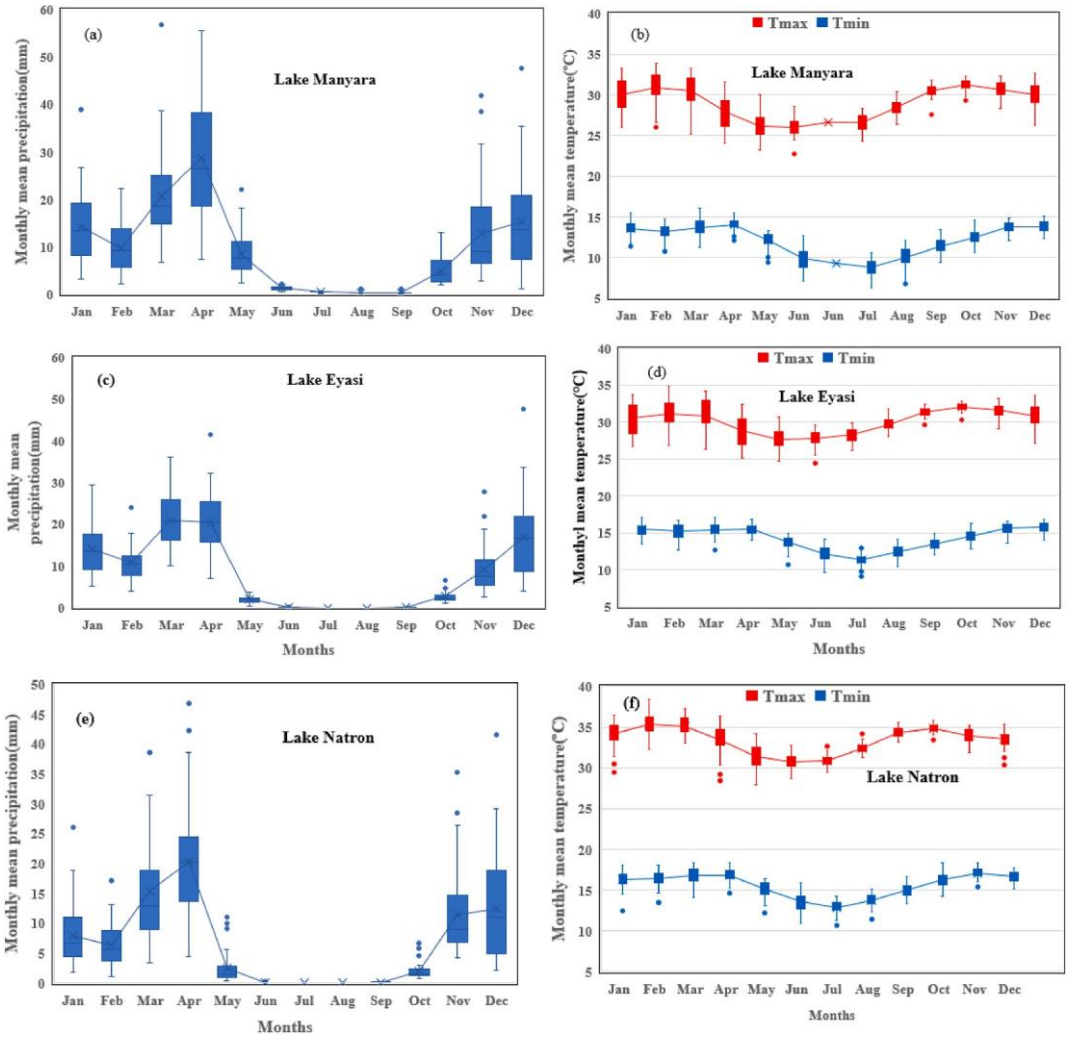

Fig. 4. The average monthly precipitation (mm) and temperatures (°C) for Lake Manyara (a and b), Lake Eyasi (c and d), and Lake Natron (e and f), respectively.

characterizing the study area. The timescale SPEI curves revealed both drying and wet episodes across the Lake basins. The negative values (red) reveal years with drought episodes due to high water scarcity, whereas the positive values (blue) indicate years with sufficient water conditions and, subsequently, wet years in the basin. The 3-month SPEI shows a higher temporal frequency of dry and wet events, although it does not reveal significant events and long-term trends. Therefore, we adopted the 6-month and 12-month timescales to discuss the drought conditions in the three lake basins as they are better suited for the detection of historically significant events and long-term impacts [72].

Across the three basins, the results indicated increasing intensities and duration of droughts over the study period. The spatio-temporal patterns of droughts exhibited a high degree of similarity across the basins, although some minor differences could be noted in some years. The SPEI results show that all the basins experienced severe drought conditions in the period 1987–1992, 2000–2010, and 2012–2017. Furthermore, the drought analysis revealed a prolonged drought between 2012 and 2017 across the studied lake basins. Since 2000, there has been an increase in the frequency of drought episodes, as supported by previous studies in the region [73–77]. On a larger scale, the drought patterns are also in line with other region-wide studies that reveal the increased prevalence of droughts and associated severities in the East Africa region and, at large, the Horn of Africa [72,78]. The prolonged drought events in recent years in the region could be due to the consequence of climate change, which disrupts the patterns of precipitation and temperature fluctuation. The increased drought events have a significant effect on the health of the various lakes, which could greatly undermine the ecosystems of the lake environments. The findings of this study are relevant to inform a delicate balance in resource utilization and environmental conservation for sustainable health of the lake systems in the region. The northern part of Tanzania is endowed with substantial water resources, which are vital for the socio-economic development of the region and the sustenance of the livelihoods in the region. Therefore, more prudent management and development of appropriate strategies and plans for water and environmental resources protection should be prioritized.

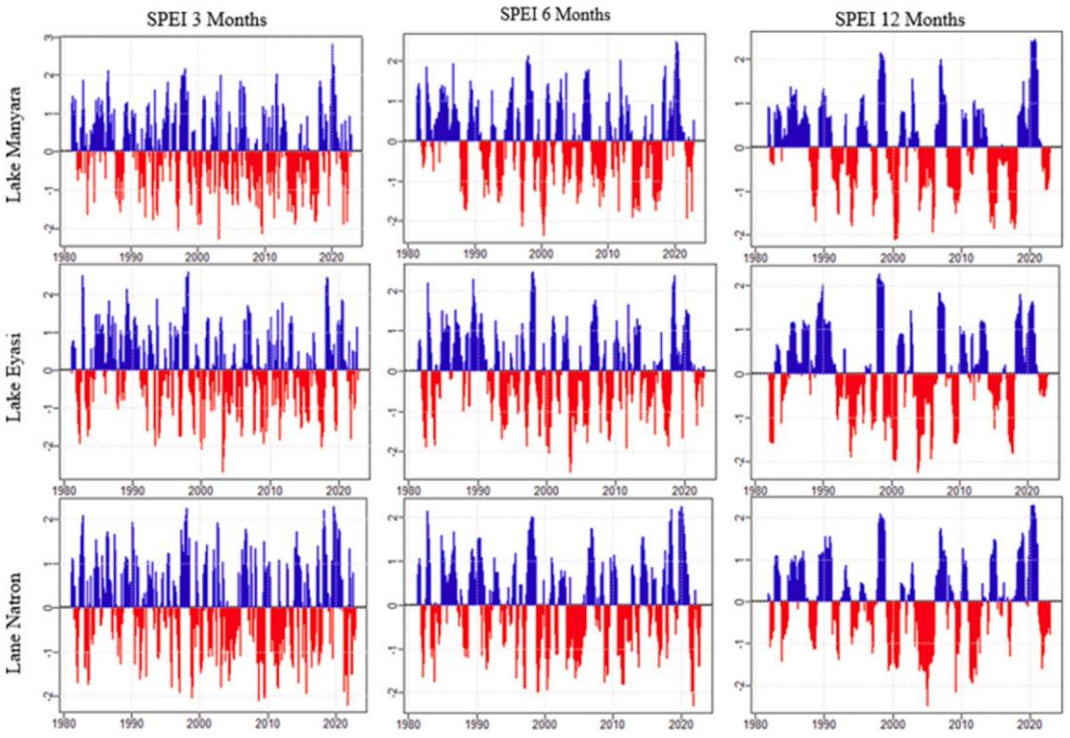

Fig. 5. The evolution of the SPEI for 3, 6, and 12-month timescales in Lake Manyara, Lake Natron, and Lake Eyasi basin shows the variation in the duration, severity, and intensity of dry and wet events.

3.4. Water quality assessment

3.4.1. Normalized Difference Water Index (NDWI)

Lake Eyasi showed increasing negative NDWI values from 2000 (—0.116) to 2014 (—0.225), indicating a reduction in water presence or surface wetness over this period (Table 2). This trend could reflect a fluctuating water level due to changing climate or anthropogenic pressures, potentially leading to increased evaporation or reduced inflow into the lake over time [44]. By 2023, the NDWI value improved slightly (—0.205), suggesting a minor increase in water volume compared to 2014, though still lower than in 2000. Lake Manyara's NDWI values similarly declined from —0.122 in 2000 to —0.205 in 2014, suggesting a decrease in surface water or higher turbidity, possibly due to sedimentation or drying trends [79]. However, like Lake Eyasi, its NDWI value in 2023 slightly increased (—0.18) relative to 2014, indicating a slight recovery in surface water or moisture content most likely due to increased precipitation.

Lake Natron showed progressively more negative NDWI values from 2000 to 2023 (Table 2). This negative shift from —0.057 to —0.119 indicates a decrease in water or surface wetness in the lake, suggesting potentially lower inflow, more evaporation, or increased sedimentation or turbidity over time. These findings align with the LULC results of the individual lakes (Fig. 9) and those by other researchers in the lake [5,46].

3.4.2. Chlorophyll Index (CI)

The CI values for the three lakes in northern Tanzania are summarized in Table 3. Lake Eyasi exhibited a steady increase in CI values, rising from 1.116 in 2000 to 1.742 in 2023. Lake Manyara showed the highest CI values among the three lakes and a consistent increase over time, from 1.276 in 2000 to 2.252 in 2023 indicating an increase in chlorophyll concentration most likely due to higher algal biomass. This increasing trend in the two lakes suggests nutrient enrichment, possibly from agricultural runoff or organic matter influx, pointing toward eutrophication driven by anthropogenic nutrient inputs as the agricultural land area expanded over the study period. According to Ref. [80] lakes can change from oligotrophic to mesotrophic, eutrophic, and finally hypertrophic due to excessive

Table 2
NDWI values of the three lakes over the study period (2000–2023).

Lake	2000	2014	2023
Eyasi	−0.116	−0.225	−0.205
Manyara	−0.122	−0.205	−0.18
Natron	−0.057	−0.112	−0.119

Table 3
Chlorophyll Index (CI) values of the three lakes over the study period (2000–2023).

Lake	2000	2014	2023
Eyasi	1.116	1.428	1.742
Manyara	1.276	1.846	2.252
Natron	1.107	1.275	1.249

nutrient enrichment exacerbated by human activities, with resultant detrimental effects on biodiversity, ecosystem functioning, and human populations.

Lake Natron had relatively stable CI values compared to the other lakes, with a slight increase from 2000 to 2014 (1.107–1.275), followed by a minor decrease by 2023 (1.249). This pattern indicates that chlorophyll levels, and hence algal productivity, have been relatively stable over time in the lake.

3.5. *Soil types classification*

Fig. 6 shows the reference soil types observed surrounding the soda-saline lakes in Northern Tanzania, with their key chemical characteristics detailed in Table 4. The soil groups identified include ferric acrisols (Af), chromic cambisols (Bc), calcic cambisols (Bk), entisols (E), inceptisols (I), eutric fluvisols (Je), distric nitisols (Nd), humic nitisols (Nh), mollic andosols (Tm), ochric andosols (To), and pellic vertisols (Vp).

The ferric acrisols (highly weathered soils) were distributed near Lake Eyasi, indicating the existence of clay soils with high iron content [81]. These ferric acrisols are formed through intense chemical weathering and are prevalent in tropical areas such as those near Lake Eyasi in Tanzania [82]. Pellic vertisols (vp) were widely distributed in the Western part of Lake Natron. This suggests that the soil has a neutral to slightly alkaline pH, significant base saturation, moderate to low organic matter, and lime accumulation, developing deep cracks during the dry season [83,84]. Additionally, in the region, we noted the presence of Entisol and Inceptsol soil orders (USDA Soil Taxonomy). Entisols are young soils with little to no horizon development [85] and are predominant in the Katesh district near Mount Hanang. In contrast, Inceptisols, with slight horizon development [85], are more widely distributed around Lake Natron and between Lakes Manyara and Eyasi. The distribution of Entisols and Inceptisols in the region suggests dynamic geological processes characterized by significant weathering and erosion [85]. Furthermore, eutric fluvisols were distributed along the lowland areas around Lakes Manyara and Eyasi. The fluvisols form from the active deposition of alluvial deposits carried by rivers and streams, typically found in river valleys, floodplains, deltas, and coastal plains [86,87]. Depending on the sediment source, fluvisols exhibit a neutral to alkaline pH, high organic matter, and nutrient content, with considerable amounts of pyrite in the subsoil [86].

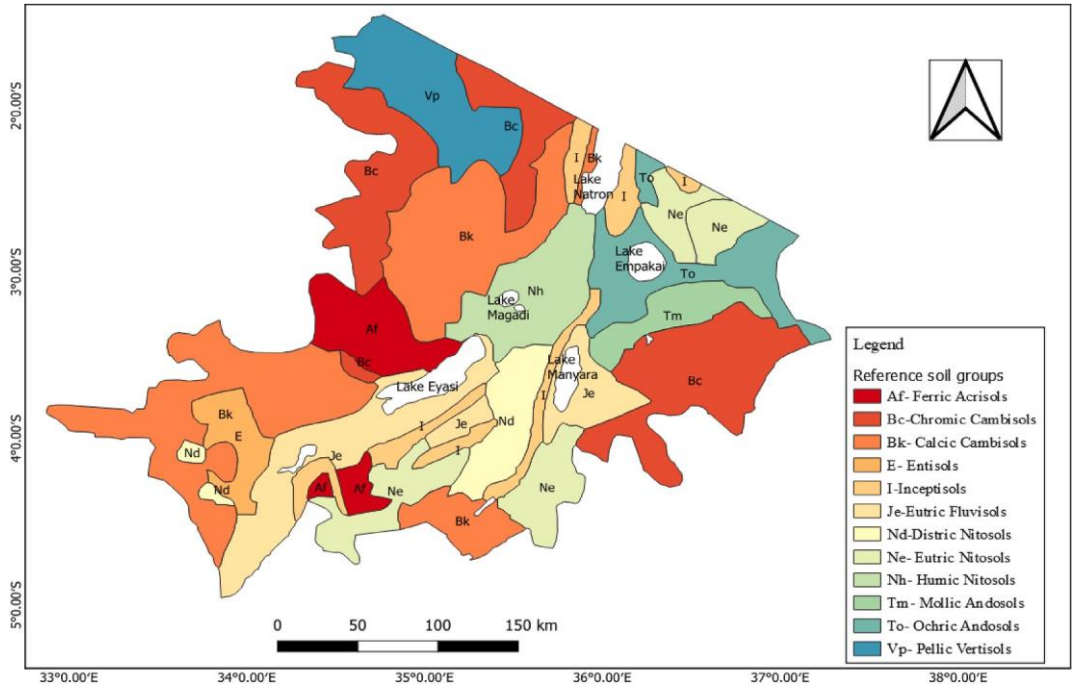

Fig. 6. Distribution of soil type in the study area extracted from the DSMW (Note, Entisol (USDA Taxonomy)/Regosol (FAO), Inceptisols (USDA Taxonomy)/Cambisol (FAO)).

Table 4
The key characteristics of the soil groups in the study area (Northern Tanzania).

soil groups	Key Characteristics	Reference
ferric acrisols	highly weathered soil rich in Fe oxides (especially rich in hematite), low-activity clays, and low base saturation, acidic soils	[92,93]
chromic cambisols and calcic cambisols	The soil profile is characterized by the presence of accumulated carbonate in the soil profile, weakly alkaline or alkaline reaction low content of humus, equal distribution of main oxides, high base saturation, Al or Fe compounds, predominant silicate iron over non-silicate iron, powerful, well-expressed carbonate - illuvial horizon	[92,93]
entisols	The soil is characterized by neutral-to-alkaline reactions, low to high base saturation, low to moderate levels of iron (Fe^{3+}) and aluminium oxides (Al^{3+}) and can accumulate calcium carbonate ($CaCO_3$)	[94]
inceptisols	The soil is characterized by neutral to slightly alkaline reactions, the clay minerals are often illite, kaolinite, or smectite, with low to moderate base saturation, moderate levels of Iron and Aluminum Oxides and contain calcium carbonate ($CaCO_3$)	[94]
eutric fluvisols	The soil forms as alluvial deposits in the river basins or lowlands, with acid, neutral or alkaline reactions, high base saturation of 50 % or more, content of silicate iron sharply predominates non-silicate iron.	[92,93]
distric nitisols and humic nitisols	The soil is associated with volcanic regions and weathered basaltic rocks, High concentrations of iron (Fe^{3+}) and aluminium (Al^{3+}) oxides, low-activity clays, rich in secondary clay minerals (especially kaolinite, and sometimes illite), high organic Matter Content, and the reaction slight acidic to neutral	[92,93]
mollic andosols and ochric andosols	The soil formed from volcanoclastic materials (volcanic ashes and ejecta), moderate to high organic matter contents, non-crystalline aluminium (Al^{3+}) and iron oxides (Fe^{3+}), and moderate to high base saturation	[92,93]
pellic vertisols	The soil profile is characterized by the humus horizon, presence of carbonate–illuvial horizon, uniform distribution of main oxides, weakly alkaline reaction, and in some cases labile soluble salts and gypsum accumulate in the soil profile.	[92,93]

In the Western part of Lake Natron and Eyasi and the eastern part of Lake Manyara, we identified the presence of chromic cambisols (Bc) and calcic cambisols, characterized by slight to moderate weathering of the parent material. Chromic cambisols exhibit a neutral to weakly acidic reaction [88], while calcic cambisols are alkaline [88]. The observed presence and distribution of mollic andosols and ochric andosols near Lake Natron, Manyara, and the Ngorongoro area indicate that volcanic activity (lavas, ash, tuffs, pumice, and other volcanic ejecta) and earthquakes [12,35] are predominant in the region. The occurrence of andosols in the study area aligns with their prevalence across Africa's rift systems [89–91]. These soils are derived from volcanic ash and other volcanic ejecta and are characterized by the presence of allophanes, imogolite, and ferrihydrite [89]. The prevalence of Andosols in the East African Rift Valley is due to the region's volcanic activity and high elevations [90,91]. The presence of andosols also suggests a history of explosive volcanic eruptions in the region, leading to the deposition of volcanic materials over time. In addition, we observed the presence of strongly weathered basaltic volcanic deposits (Nitisols) in the region. Humic nitisols are widespread across the Ngorongoro crater, influencing the alkalinity of Lake Magadi [35]. Distric nitisols are widely distributed between Lake Manyara and Eyasi and in the Katesh area of Mount Hanang. The distribution of the nitisol soil type highlights geological complexity and the predominance of volcanic activity in the region. The diverse soil types in the region play a critical role in shaping the chemistry of the surrounding

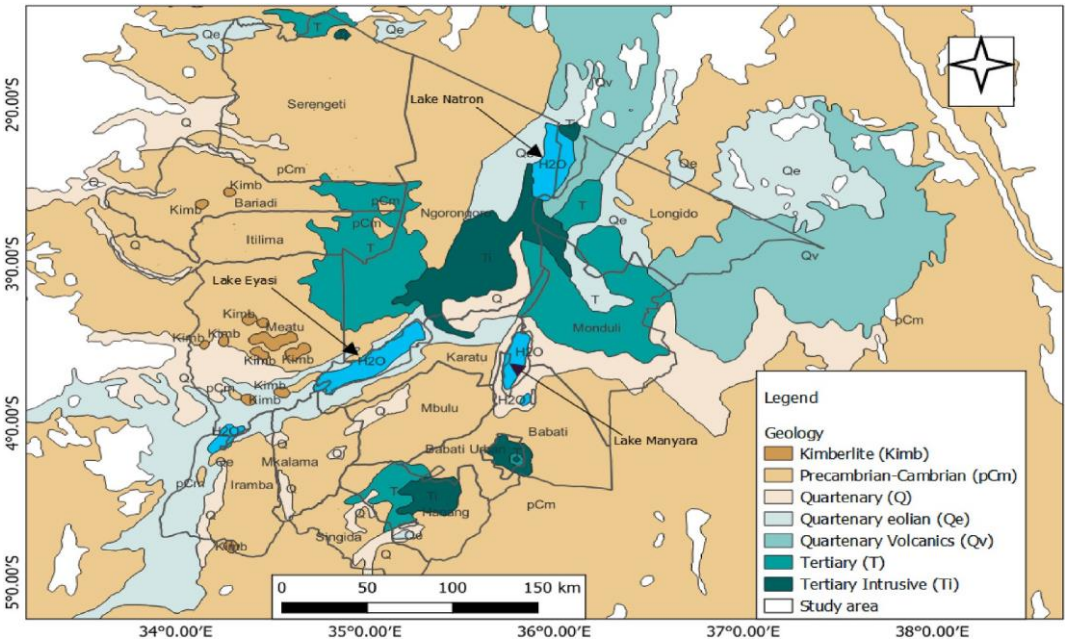

Fig. 7. The geological map of the study area generated from the World Geological Map USGS database.

soda-saline lakes. Each type originates from different parent materials and exhibits distinct chemical characteristics. The interaction of the lake water with the soil groups through weathering and dissolution introduces key chemical constituents to the lakes that influence the lake's water chemistry. The leaching, runoff, and sediment deposition processes, release dissolved ions and minerals into the water and contribute to higher alkalinity of soda and soda-saline lakes. Soils rich in carbonates, such as Chromic and Calcic Cambisols, Entisols, and Inceptisols, contribute to the alkalinity of these lakes by providing carbonate ions, which buffer the pH and maintain high alkalinity. Soils with high base saturation and weakly alkaline reactions, like Eutric Fluvisols and Pellic Vertisols, supply essential salts and ions, promoting the saline conditions typical of soda-saline lakes. Volcanic soils like Andosols and Nitisols, add volcanic mineral contents and contribute to higher alkalinity of the soda and soda-saline lakes. Alkaline and carbonate-rich soils directly correlate with the high pH and salinity of soda and soda-saline lakes, while soils with volcanic or high iron content influence the mineral composition. The interaction of lake water and these soil types creates a dynamic balance in the lake's pH, alkalinity and nutrient dynamics, leading to variations in primary productivity, algal growth, and overall lake ecosystem health.

3.6. Geological features

The geological attributes of the areas surrounding the soda and soda-saline lakes in northern Tanzania are depicted in Fig. 7, and the key chemical constituents are detailed in Table 5. The map reveals diverse geological features, including Kimberlite (Kimb), Precambrian-Cambrian (pCm), Quaternary (Q), Quaternary Eolian (Qe), Quaternary Volcanics (Qv), Tertiary (T), and Tertiary Intrusive (Ti).

Kimberlite mineral deposits are distributed in clusters in the western parts near Lake Eyasi in the Meatu and Bariadi districts. Kimberlite igneous rock contains a variety of minerals, including olivine, mica, serpentine, calcite, monticellite, apatite, and smaller amounts of dolomite, phlogopite, spinel, perovskite, and ilmenite [95–98]. The composition of olivines and spinel is dominated by dolomite, calcite, and alkali carbonates, with a smaller amount of silicate and oxide minerals [98,99]. Olivine secondary inclusions host an assemblage of Na-K carbonates and chloride [98]. Weathering of kimberlite mineral deposits contributes alkali carbonates and silicates, which raise sodium and potassium levels in the lakes, enhancing the alkaline nature of the soda and soda-saline lakes.

The extensive coverage of Precambrian-Cambrian (pCm) rocks observed in the Western, Southern, and Eastern regions indicates stable geological conditions during the transition from the Precambrian to the Cambrian period, marked by consistent sediment deposition. Precambrian rocks, including intrusive granitic and volcanic rocks, feature minerals such as feldspar, pyroxene, microcrystalline quartz, olivine, calcium carbonates, iron carbonates, dolomites, and magnesite [100–102]. Precambrian rocks, rich in calcium carbonates and silicates, provide carbonate ions that help maintain high pH and support the formation of soda minerals like trona which correlates to the trona formation in the soda lakes. Cambrian sediments, comprising basal conglomerates, sandstone, and siltstone, contain quartz, moganite, calcite, dolomite, feldspar, phyllosilicates, zircon, monazite, uranophane, thoriante, xenotime, pyrite, and gold [100,102]. Cambrian sediments, containing quartz, dolomite, and feldspar, supply additional carbonate and silicate minerals, further contributing to the alkaline environment of the soda and soda-saline lake.

Quaternary (Q) formations are found in scattered patches around Lake Manyara, Eyasi, and the southern part of the region, while Quaternary Volcanic (Qv) formations are primarily distributed in the Eastern part of Lake Natron, Southeastern Longido, and Eastern Monduli districts. This distribution indicates significant volcanic activity and sedimentary deposits from the Quaternary period. Quaternary Eolian (Qe) formations were found in patches, particularly in the western part of Lake Natron, the western areas of Longido and Monduli districts, and the southern part of the Eyasi rift. This suggests that wind deposition is actively shaping the landscape in the region. Tertiary (T) formations are distributed in the Monduli districts northeast of Lake Manyara, Southwest of Lake Eyasi, and on Mount Hanang in the Katesh districts. Tertiary intrusive (Ti) formations are primarily located in the Ngorongoro Crater in the Southern region of Lake Natron, extending towards Lake Eyasi in the North, with smaller portions found in the Northern part of Lake Natron and on Mount Hanang in the Katesh districts. Our observations align with the previous study's reported dominance of volcanic and tectonic activity in the region [12,47–51]. The presence and distribution of quaternary to tertiary intrusive volcanoes indicate active tectonic and volcanic activity in the region. Evidence of this ongoing volcanic activity includes the natrocarbonatite volcanoes, such as Oldonyo Lengai, and distinct geological features like cinder cones, lava flows, mudflows, pyroclastic flows, pumice, and volcanic ash [33,47,48,

Table 5
The geological features and key chemical constituents in the study area (Northern Tanzania).

Geological features	rock minerals	Key Chemical Constituents	Reference
Kimberlite mineral deposits	olivine, mica, serpentine, calcite, monticellite, apatite, and smaller amounts of dolomite, phlogopite, spinel, perovskite, and ilmenite	alkali carbonates (Na-K carbonates), chloride, silicate and oxide minerals	[95–98]
Precambrian rocks	intrusive granitic and volcanic rocks	feldspar, pyroxene, microcrystalline quartz, olivine, calcium carbonates, iron carbonates, dolomites, and magnesite	[100–102].
Cambrian sediments		basal conglomerates, sandstone, and siltstone, contain quartz, moganite, calcite, dolomite, feldspar, phyllosilicates, zircon, monazite, uranophane, thoriante, xenotime, pyrite, gold	[100,102]
quaternary to tertiary intrusive volcanoes	natrocarbonatite volcanoes (cinder cones, lava flows, mudflows, pyroclastic flows, pumice, and volcanic ash)	alkali carbonate minerals, such as nahcolite ($NaHCO_3$), trona ($Na_3H(CO_3)_2{\cdot}2H_2O$), thermonatrite ($Na_2CO_3{\cdot}H_2O$), pirssonite ($CaCO_3{\cdot}Na_2CO_3{\cdot}2H_2O$), gaylussite ($CaCO_3{\cdot}Na_2CO_3{\cdot}5H_2O$), and calcite ($CaCO_3$)	[33,47,48, 50]

50]. The primary volcanic deposits in the region consist of alkali carbonate minerals, such as $Na_2Ca(CO_3)_2$ and Na_2CO_3 [33], which greatly influence the chemistry of the soda-saline lakes. The interaction between volcanic materials and lake waters contributes to the lakes' unique chemical composition, characterized by high alkalinity and distinctive ecological conditions [18,19]. The influence of volcanic activity, particularly from natrocarbonatite volcanoes, is significant, as they release large amounts of sodium carbonate minerals such as trona and nahcolite into the lakes. The continuous input of volcanic gases and minerals into these lakes plays a vital role in shaping the physical landscape and maintaining the ecological diversity and unique c alkaline water chemistry of the soda-saline lakes.

3.7. Land use and land cover (LULC) changes

3.7.1. Accuracy statement

The overall accuracies were above 80 % while the Kappa coefficients were greater than 0.70 (Table 6). These results were within the acceptable range; therefore, we proceeded to use the classification outputs [65,103].

3.7.2. LULC and lake areas statistics and maps

The LULC classes showed spatial and temporal variations, as seen in Table 7 and Fig. 8. In 2000 and 2014, bareland covered most of our study area (58.73 % and 50.77 %), while shrubs and grasses comprised the second largest LULC type (21.80 % and 33.47 %) respectively. As of 2023 shrubs and grasses dominated the study area (37.66 %) which is closely followed by bareland (37.48 %). Built-up areas formed the least cover of the study area for all three years. Water bodies covered the second smallest area (5.07 %, 2.87 % and 3.05 %) throughout the study years (Table 7).

The analysis of the individual lakes revealed that Lake Eyasi had the largest area coverage across all three study years, as shown in Table 8. In contrast, Lake Manyara had the smallest area in both 2000 (54,873.81 ha) and 2014 (21,760.61 ha). By 2023, however, Lake Natron had the smallest area (20,368.59 ha) indicating distinct patterns of area change among the lakes over time. In 2014, both Lakes declined in their catchment areas, as shown in Fig. 9. This reduction may be attributed to the prolonged droughts between 2000 and 2017, as depicted in Fig. 5. The extended periods of drought likely played a significant role in reducing precipitation, and water inflow, leading to the observed shrinkage in lake size during this period.

Regarding spatial distribution, water bodies were located in the southern and northern parts of the study area, forest in the central, shrubs and grasses in the south and southwest, agricultural lands in the southeast and bare lands throughout the study area (Fig. 8). These classes displayed variations in cover over time, contributing to the changes in the chemistry of the lakes.

The spatial and temporal variations of the individual lakes are displayed in Fig. 9.

3.7.3. LULC and lake changes

There were dynamics in the areas of the numerous LULC classes over time as shown in Table 9. During the first study period (2000–2014), there was a substantial drop in forest areas (—45.15 %), water bodies (—43.39 %), as well as bareland (—13.56 %). On the other hand, areas under agricultural land (17.04 %), built-up areas (384.63 %), and shrubs and grasses (53.54 %) increased. In the second period (2014–2023), all LULC classes except bareland increased in area (Table 9). Overall (2000–2023), there was a decrease in areas under water bodies (—39.80 %), forests (—22.57 %) and bareland (—36.18) while agricultural land (111.01 %) built-up areas (434.72 %), shrubs and grasses (72.77 %) increased. Previous studies using RS in the Urmia Lake basin in Northwestern Iran and Lake Naivasha in Kenya have similarly shown an increase in agricultural lands and urban/built-up areas, with a corresponding decrease in the lake/water bodies area largely due to anthropogenic activities and climatic changes [104,105].

The expansion of built-up areas in our study area can be linked to population increase over the years [106]. The population increase subsequently results in agricultural expansion and intensification to meet the food and commercial demands of the population [107]. An increase in agricultural activities is often associated with increased water abstraction through irrigation and the use of inorganic fertilizers, pesticides and herbicides which eventually alter the chemical composition of the water bodies in addition to promoting algal bloom [36,108]. Population increase also translates to an increase in domestic and commercial effluent discharge which results in water resources contamination. Earlier research has also shown anthropogenic alterations as the leading cause of significant changes in land use and water storage for most lakes [105]. There was a notable decrease in the forest cover in the study area over the two decades most likely due to anthropogenic activities. Deforestation and forest degradation expose soils and rocks to weathering and erosion, resulting in increased sediment loads and nutrient inputs into lake waters thereby altering their chemical compositions [40].

A further analysis of the individual lakes also showed changes in their area coverage between the study years. Lake Natron steadily decreased between 2000–2014 and 2014–2023 while Lakes Eyasi and Manyara likewise decreased between 2000 and 2014 but later increased between 2014 and 2023 (Table 7). Overall, negative area changes were recorded for Lake Natron (—52,964.31 ha) and Lake Eyasi (—46,805.76 ha) while a positive area change was noted for Lake Manyara (162.36 ha) (Table 10). The reductions in lake surface areas can be linked to water abstraction [109] and climate variability [110], which have had a considerable effect on water volumes.

Table 6
Accuracy assessment.

	2000	2014	2023
Overall accuracy	92.55	84.59	81.57
Kappa hat	0.87	0.75	0.72

Table 7
LULC areas and percentages for 2000, 2014 and 2023.

LULC Class	2000		2014		2023	
	Area (ha)	Area (%)	Area (ha)	Area (%)	Area (ha)	Area (%)
Water bodies	262304.42	5.07	148491.07	2.87	157900.61	3.05
Forest	334007.72	6.46	183211.33	3.54	258615.37	5.00
Shrubs & grasses	1127623.3	21.8	1731349.05	33.47	1948192.3	37.66
Bareland	3037905.51	58.73	2626045.29	50.77	1938675.6	37.48
Agricultural land	410050.59	7.93	479914.71	9.28	865253.47	16.73
Built up	748.8	0.01	3628.89	0.07	4003.99	0.08
Total	**5172640.34**	**100**	**5172640.34**	**100**	**5172641.34**	**100**

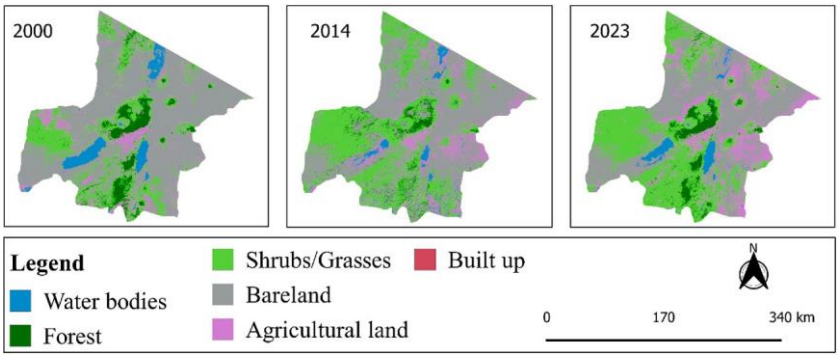

Fig. 8. Map showing the spatial distribution of the various LULC classes over the study period.

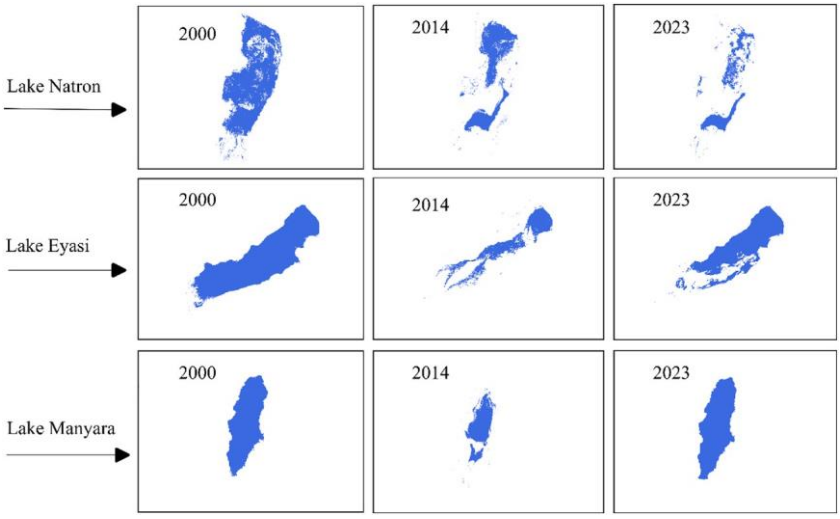

Fig. 9. Maps showing the spatio-temporal dynamics of the three lakes in the study area.

Table 8
Individual Lakes statistics for 2000, 2014 and 2023 in the study area.

Lake name	2000	2014	2023
	Area (ha)	Area (ha)	Area (ha)
Lake Natron	73332.90	34970.02	20368.59
Lake Eyasi	115284.80	35788.93	68479.04
Lake Manyara	54873.81	21760.61	55036.17

Table 9
LULC changes between the study years.

LULC class	2000–2014		2014–2023		2000–2023	
	ha	%	ha	%	ha	%
Water bodies	−113813.35	−43.39	9409.54	6.34	−104403.81	−39.8
Forest	−150796.39	−45.15	75404.04	41.16	−75392.35	−22.57
Shrubs & grasses	603725.75	53.54	216843.25	12.52	820569	72.77
Bareland	−411860.22	−13.56	−687369.69	−26.18	−1099229.91	−36.18
Agricultural land	69864.12	17.04	385338.76	80.29	455202.88	111.01
Built up	2880.09	384.63	375.1	10.34	3255.19	434.72

Table 10
Changes in individual Lake area coverage between the study years.

Lake name	2000–2014	2014–2023	2014–2023
	Area (ha)	Area (ha)	Area (ha)
Lake Natron	−38,362.88	−14,601.43	−52,964.31
Lake Eyasi	−79,495.87	32,690.11	−46,805.76
Lake Manyara	−33,113.20	33,275.56	162.36

These decreases in volume, in turn, influence the dynamic water chemistry of the lakes by altering the concentration of dissolved minerals and other key chemical elements, thereby affecting the overall ecological balance and health of the lake ecosystems.

Our results align with a time series study of Lake Natron's surface area between 1984 and 2011 which similarly showed a high degree of variability in the lake levels due to climate variability and catchment degradation [5]. A mixed-method approach, involving a multidisciplinary stakeholders' engagement identified decreasing water levels, human activities near the lake, siltation and evaporation as the key challenges facing Lake Manyara [79]. A study of Eastern Rift Valley Lakes in Northern Tanzania comprising the three lakes (Natron, Eyasi, Manyara) among others also linked the fluctuations in lake water levels to geologic, climatic, and biological events occurring within and outside the lake [111].

4. Conclusions

This study explores the complex interactions between environmental factors, human activities, and the chemical composition of soda-saline lakes in Northern Tanzania using remote sensing (RS) and geographical information systems (GIS) approaches. The findings revealed that the region is characterized by climate variability, with extended droughts between 2000 and 2017. This suggests that climate variability and drought events in the region can lead to increased evapotranspiration, shaping the chemistry of soda and soda-saline lakes. The region's diverse soil types, including ferric acrisols, chromic cambisols, calcic cambisols, entisols, inceptisols, eutric fluvisols, distric nitisols, humic nitisols, mollic andosols, ochric andosols, and pellic vertisols. Additionally, geological processes in the region ranged from the Precambrian-Cambrian to Tertiary Intrusive periods, driven by volcanic and tectonic activity. The region's diverse soil mineralogy and volcanic activity suggest that soil and volcanic activities are key drivers in introducing unique chemical components through weathering and erosion, affecting the lakes' alkalinity, salinity, and pH. The study also reveals significant land use/land cover (LULC) changes over the 23 years (2000–2023), including reductions in water bodies, forests, and bareland, alongside increases in agricultural land, built-up areas, and shrubs and grasses. A more detailed analysis of the individual lakes revealed notable changes in their area coverage. Lake Natron experienced a consistent decline in size during both periods, from 2000 to 2014 and 2014–2023. In contrast, Lakes Eyasi and Manyara also saw a reduction in the area between 2000 and 2014, but unlike Lake Natron, both lakes showed a reversal in this trend, with their areas expanding between 2014 and 2023. This variation highlights the differing hydrological responses, catchment degradation, siltation and evaporation of these lakes over time, providing valuable insights into their distinct environmental dynamics. Understanding the dynamic interactions of the environmental variables and anthropogenic is essential for developing effective conservation and management strategies to protect the ecological health of soda-saline lakes. Implementing sustainable land use practices and minimizing pollution is key to preserving biodiversity and maintaining water quality for future generations.

5. Limitations of the study

While this study provides valuable insights into the environmental and human factors influencing soda-saline lake chemistry, several limitations should be acknowledged:

1. The study primarily relies on satellite-based data due to the unavailability of on-site station data. Although useful for large-scale observations, satellite data may lack the resolution needed to capture finer, short-term variations in climate.

2. The study does not account for future climate change projections, which limits its ability to predict long-term impacts on lake ecosystems and water chemistry. Incorporating future projections could provide a more comprehensive understanding of potential future changes.
3. While the study addresses land use changes driven by human activities, it does not include an analysis of chemical pollutants generated from anthropogenic sources. Assessing the levels and types of pollutants entering the lakes from anthropogenic sources would provide a clearer picture of human impact on lake chemistry.
4. The GIS-based soil and geology classifications may have inherent limitations which require field and ground data validation.
5. The study lacks data on the chemical composition of the soils and geological formations surrounding the lakes. Including this information could provide a more detailed understanding of how local soil and geology influence the lakes' chemical profiles.

Addressing these limitations in future research could significantly improve the precision and depth of insights into the environmental and human-induced factors affecting soda-saline lakes.

CRediT authorship contribution statement

Azaria Stephano Lameck: Writing – review & editing, Writing – original draft, Methodology, Conceptualization. **Brian Rotich:** Writing – review & editing, Writing – original draft. **Abdalrahman Ahmed:** Writing – review & editing, Writing – original draft, Visualization, Methodology, Investigation, Formal analysis. **Harison K. Kipkulei:** Writing – review & editing, Writing – original draft, Methodology. **Peto Akos:** Writing – review & editing. **Emil Boros:** Writing – review & editing.

Data availability statement

Data will be made available on request.

Ethical statement

The authors of this study affirm that the research was carried out following ethical guidelines and regulations.

Funding

None.

Declaration of competing interest

The authors declare that they have no known competing financial interests or personal relationships that could have appeared to influence the work reported in this paper.

Acknowledgement

The authors of this article would like to sincerely thank reviewers for their valuable time and expertise in offering insightful comments and constructive criticism to enhance the quality of this work. Their contributions have been instrumental in shaping the final version of this article, and we are truly thankful for their support.

References

[1] E. Boros, M. Kolpakova, A review of the defining chemical properties of soda lakes and pans: an assessment on a large geographic scale of Eurasian inland saline surface waters, PLoS One 13 (2018) 1–20, https://doi.org/10.1371/journal.pone.0202205.
[2] W.D. Grant, Alkaline environments and biodiversity, in: C. Gerday, N. Glansdorff (Eds.), Extrem. Handb., Eolss Publishers, Oxford, UK, Uk, 2006, pp. 21–24. http://www.eolss.net.
[3] W.D. Grant, B.E. Jones, Bacteria, archaea and viruses of soda lakes, in: M. Schagerl (Ed.), Soda Lake East Africa, Springer International Publishing Switzerland, 2016, pp. 97–148, https://doi.org/10.1007/978-3-319-28622-8_5.
[4] B.E. Jones, W.D. Grant, A.W. Duckworth, G.G. Owenson, Microbial diversity of soda lakes, Extremophiles 2 (1998) 191–200, https://doi.org/10.1007/s007920050060.
[5] E.J. Tebbs, J.J. Remedios, S.T. Avery, D.M. Harper, Remote sensing the hydrological variability of Tanzania ' s Lake Natron , a vital Lesser Flamingo breeding site under threat, Ecohydrol. Hydrobiol. 13 (2013) 148–158, https://doi.org/10.1016/j.ecohyd.2013.02.002.
[6] J.V. Robinson, The Ecology of East African Soda Lakes : Implications for Lesser Flamingo (Phoeniconaias Minor) Feeding Behaviour Thesis Submitted for the Degree of Doctor of Philosophy at the University of Leicester by, 2015.
[7] M. Schagerl, A. Burian, The ecology of African soda lakes: driven by variable and extreme conditions, Soda Lakes East Africa 12 (2016) 1–408, https://doi.org/10.1007/978-3-319-28622-8.
[8] D.Y. Sorokin, T.P. Tourova, A.M. Henstra, A.J.M. Stams, E.A. Galinski, G. Muyzer, Sulfidogenesis under extremely haloalkaline conditions by Desulfonatronospira thiodismutans gen. nov., sp. nov., and Desulfonatronospira delicat sp. nov. - a novel lineage of Deltaproteobacteria from hypersaline soda lakes, Microbiology 154 (2008) 1444–1453, https://doi.org/10.1099/mic.0.2007/015628-0.
[9] D.Y. Sorokin, T. Berben, E.D. Melton, L. Overmars, C.D. Vavourakis, G. Muyzer, Microbial diversity and biogeochemical cycling in soda lakes, Extremophiles 18 (2014) 791–809, https://doi.org/10.1007/s00792-014-0670-9.
[10] D.Y. Sorokin, H.L. Banciu, G. Muyzer, Functional microbiology of soda lakes, Curr. Opin. Microbiol. 25 (2015) 88–96, https://doi.org/10.1016/j.mib.2015.05.004.

[11] R.M.J. Kadigi, F. Kilima, J. Kashaigili, A Comparative Study of Costs and Benefits of Soda Ash Mining and Promotion of Ecotourism and Sustainable Use of Natural Resources in Lake Natron Basin, Tanzania, 2013.
[12] R.N. Scoon, Geotourism, iconic landforms and island-style speciation patterns in national parks of East Africa, Geoheritage 12 (2020), https://doi.org/10.1007/s12371-020-00486-z.
[13] A. stephano Lameck, O. Saeed, E. Boros, The chemical composition , classification , and geographical distributions of soda-saline lakes in Eastern Tanzania ' s rift valley, J. Hydrol. Reg. Stud. 51 (2024) 101668, https://doi.org/10.1016/j.ejrh.2024.101668.
[14] H. Rahimpour, A. Fahmi, S. Zinatloo-ajabshir, Results in Engineering toward sustainable soda ash production : a critical review on eco-impacts , modifications , and innovative approaches, Results Eng 23 (2024) 102399, https://doi.org/10.1016/j.rineng.2024.102399.
[15] Jozsef Toth, Groundwater as a geologic agent : an overview of the causes , processes , and manifestations, Hydrogeol. J. 7 (1999) 1–14.
[16] E.N. Bui, Causes of soil salinization, sodification, and alkalinization, Oxford Res. Encycl. Environ. Sci. (2017) 1–25, https://doi.org/10.1093/acrefore/9780199389414.013.264.
[17] H. Melese, H.J. Debella, Comparative study on seasonal variations in physico-chemical characteristics of four soda lakes of Ethiopia (Arenguade, Beseka, Chitu and Shala), Heliyon 9 (2023) e16308, https://doi.org/10.1016/j.heliyon.2023.e16308.
[18] G. Pecoraino, W. Alessandro, S. Inguaggiato, The other side of the coin: geochemistry of alkaline lakes in volcanic areas, Volcan. Lakes (2015) 219–237, https://doi.org/10.1007/978-3-642-36833-2.
[19] D.M. Deocampo, R.W. Renaut, Geochemistry of African soda lakes, Soda Lakes East Africa (2016) 77–93, https://doi.org/10.1007/978-3-319-28622-8.
[20] F. Frondini, W. Dragoni, N. Morgantini, M. Donnini, C. Cardellini, S. Caliro, M. Melillo, G. Chiodini, An endorheic lake in a changing climate :geochemical investigations at lake trasimeno (Italy), Water 11 (2019).
[21] J.C. Evans, E.E. Prepas, Potential effects of climate change on ion chemistry and phytoplankton communities in prairie saline lakes, Limnol. Oceanogr. 41 (1996) 1063–1076, https://doi.org/10.4319/lo.1996.41.5.1063.
[22] K.E. Strock, J.E. Saros, S.J. Nelson, S.D. Birkel, J.S. Kahl, W.H. McDowell, Extreme weather years drive episodic changes in lake chemistry: implications for recovery from sulfate deposition and long-term trends in dissolved organic carbon, Biogeochemistry 127 (2016) 353–365, https://doi.org/10.1007/s10533-016-0185-9.
[23] T.E. Cerling, Paleochemistry of plio-pleistocene lake Turkana, Kenya, Palaeogeogr. Palaeoclimatol. Palaeoecol. 27 (1979) 247–285, https://doi.org/10.1016/0031-0182(79)90105-6.
[24] M.P. Lebedeva Verba, O.V. Lopukhina, N.V. Kalinina, Specificity of the chemical and mineralogical composition of salts in solonchak playas and lakes of the Kulunda steppe, Eurasian Soil Sci. 41 (2008) 416–428, https://doi.org/10.1134/S106422930804008X.
[25] W.A. Wurtsbaugh, C. Miller, S.E. Null, R. Justin De Rose, P. Wilcock, M. Hahnenberger, F. Howe, J. Moore, Decline of the world's saline lakes, Nat. Geosci. 10 (2017) 816–821, https://doi.org/10.1038/NGEO3052.
[26] M. Sojka, A. Choinski, M. Ptak, M. Siepak, The variability of Lake water chemistry in the bory, Water (2020) 12.
[27] A.M. Desellas, A.M. Paterson, K.M. Rühland, J.P. Smol, Lake water chemistry and its relationship to shoreline residential development and natural landscape features in Algonquin Provincial Park, Ontario, Canada, Can. J. Fish. Aquat. Sci. 81 (2024) 137–153, https://doi.org/10.1139/cjfas-2023-0103.
[28] W. Wang, W. Li, M. Xue, X. Gu, C. Ye, Y. Jiao, B. Liu, Y. Han, Y. Tong, X. Zhang, Spatial-temporal characteristics and influencing factors of Lake water and groundwater chemistry in hulun lake, northeast China, Water (Switzerland) 15 (2023), https://doi.org/10.3390/w15050937.
[29] K.A. Chikita, K. Amita, H. Oyagi, J. Okada, Effects of a volcanic-fluid cycle system on water chemistry of a deep caldera lake: lake tazawa, Akita Prefecture, Japan, Water (Switzerland) 14 (2022), https://doi.org/10.3390/w14193186.
[30] P.V. Mosquera, H. Hampel, R.F. Va´zquez, J. Catalan, Water chemistry variation in tropical high-mountain lakes on old volcanic bedrocks, Limnol. Oceanogr. 67 (2022) 1522–1536, https://doi.org/10.1002/lno.12099.
[31] B.F. Jones, H.P. Eugster, S.L. Rettig, Hydrochemistry of the Lake Magadi basin, Kenya, Geochim. Cosmochim. Acta 41 (1977) 53–72, https://doi.org/10.1016/0016-7037(77)90186-7.
[32] B. Gizaw, The origin of high bicarbonate and fluoride concentrations in waters of the Main Ethiopian Rift Valley, East African Rift system, J. Afr. Earth Sci. 22 (1996) 391–402, https://doi.org/10.1016/0899-5362(96)00029-2.
[33] A.N. Zaitsev, J. Keller, Mineralogical and chemical transformation of Oldoinyo Lengai natrocarbonatites, Tanzania, Lithos 91 (2006) 191–207, https://doi.org/10.1016/j.lithos.2006.03.018.
[34] G.F. Mollel, C.C. Swisher, M.D. Feigenson, M.J. Carr, Geochemical evolution of Ngorongoro caldera, northern Tanzania: implications for crust-magma interaction, Earth Planet Sci. Lett. 271 (2008) 337–347, https://doi.org/10.1016/j.epsl.2008.04.014.
[35] D.M. Deocampo, Hydrogeochemistry in the Ngorongoro Crater, Tanzania, and implications for land use in a world heritage site, Appl. Geochem. 19 (2004) 755–767, https://doi.org/10.1016/j.apgeochem.2003.10.006.
[36] I. Zahoor, A. Mushtaq, Water pollution from agricultural activities: a critical global review, Int. J. Chem. Biochem. Sci. 23 (2023) 164–176.
[37] I. McVey, A. Michalek, T. Mahoney, A. Husic, Urbanization as a limiter and catalyst of watershed-scale sediment transport: insights from probabilistic connectivity modeling, Sci. Total Environ. 894 (2023) 165093, https://doi.org/10.1016/j.scitotenv.2023.165093.
[38] K.M. MacKenzie, K. Singh, A.D. Binns, H.R. Whiteley, B. Gharabaghi, Effects of urbanization on stream flow, sediment, and phosphorous regime, J. Hydrol. 612 (2022) 128283, https://doi.org/10.1016/j.jhydrol.2022.128283.
[39] X. Kong, S. Ghaffar, M. Determann, K. Friese, S. Jomaa, C. Mi, T. Shatwell, K. Rinke, M. Rode, Reservoir water quality deterioration due to deforestation emphasizes the indirect effects of global change, Water Res. 221 (2022) 118721, https://doi.org/10.1016/j.watres.2022.118721.
[40] W.W. Hay, Detrital sediment fluxes from continents to oceans, Chem. Geol. 145 (1998) 287–323, https://doi.org/10.1016/S0009-2541(97)00149-6.
[41] S.A. Lameck, J. Skutai, E. Boros, Review of chemical properties of inland soda and saline waters in East Africa (rift valley region), J. Hydrol. Reg. Stud. 46 (2023) 101323, https://doi.org/10.1016/j.ejrh.2023.101323.
[42] R.E. Hecky, P. Kilham, Diatoms in alkaline, saline lakes: ecology and geochemical implications, Limnol. Oceanogr. 18 (1973) 53–71, https://doi.org/10.4319/lo.1973.18.1.0053.
[43] B. Fritz, M.-P. Zins-Pawlas, M. Gueddari, Geochemistry of silica-rich brines from Lake Natron (Tanzania). Ge´ochimie des saumures riches en silice du lac Natron (Tanzanie), Sci. Ge´ologiques. Bull. 40 (1987) 97–110, https://doi.org/10.3406/sgeol.1987.1753.
[44] D.M. Deocampo, Evaporative Evolution of Surface Waters and the Role of Aqueous CO2 in Magnesium Silicate Precipitation: Lake Eyasi and Ngorongoro Crater, Northern Tanzania, vol. 108, 2005, pp. 493–504, https://doi.org/10.2113/108.4.493.
[45] E.F. Mgimwa, J.R. John, C. V Lugomela, The influence of physical – - chemical variables on phytoplankton and lesser flamingo (Phoeniconaias minor) abundances in Lake, Afr. J. Ecol. 59 (2021) 667–675, https://doi.org/10.1111/aje.12863.
[46] C. Yona, M. Makange, E. Moshiro, A. Chengula, G. Misinzo, Water pollution at Lake Natron Ramsar site in Tanzania : a threat to aquatic life, Ecohydrol, Hydrobiol. (Sofia) (2022) 1–11, https://doi.org/10.1016/j.ecohyd.2022.11.001.
[47] J.B. Dawson, The Gregory Rift Valley and Neogene-Recent Volcanoes of Northern Tanzania, Geological Society of, London, 2008.
[48] J.B. Dawson, Aspects of Rift Valley faulting and volcanicity in North Tanzania: report of a geologists' association field meeting in 2008, Proc. Geol. Assoc. 121 (2010) 342–349, https://doi.org/10.1016/j.pgeola.2010.06.003.
[49] J. Biggs, M. Chivers, M.C. Hutchinson, Surface deformation and stress interactions during the 2007-2010 sequence of earthquake, dyke intrusion and eruption in northern Tanzania, Geophys. J. Int. 195 (2013) 16–26, https://doi.org/10.1093/gji/ggt226.
[50] B.D.R. Sherrod, M.M. Magigita, S. Kwelwa, Geologic map of Oldonyo Lengai volcano and surroundings, Arusha region, United Republic of Tanzania, USGS Rep (2013) 1–61.
[51] R.N. Scoon, Geology of national parks of central/southern Kenya and northern Tanzania: geotourism of the gregory Rift Valley, active volcanism and regional plateaus. https://doi.org/10.1007/9783319737850, 2018.

[52] M. Mwabumba, B.K. Yadav, M.J. Rwiza, I. Larbi, S.Q. Dotse, A.M. Limantol, S. Sarpong, D. Kwawuvi, Rainfall and temperature changes under different climate scenarios at the watersheds surrounding the Ngorongoro Conservation Area in Tanzania, Environ. Challenges 7 (2022) 100446, https://doi.org/10.1016/j.envc.2022.100446.

[53] A.M. Catherine, M. Revocatus, S. Hussein, Will Ngorongoro Conservation Area remain a world heritage site amidst increasing human footprint? Int. J. Biodivers. Conserv. 7 (2015) 394–407, https://doi.org/10.5897/ijbc2015.0837.

[54] A.Z. Lawuo, B. Mbasa, Stephen Mnyawi, Persistence of land conflicts between Maasai community and Ngorongoro conservation area authority (Ncaa) in Ngorongoro conservation area (Nca), Int. J. Innov. Sci. Res. 5 (2014) 154–161. http://www.ijisr.issr-journals.org/.

[55] J.B. Dawson, The Gregory Rift Valley and Neogene-Recent Volcanoes of Northern Tanzania, Geol. Soc. London, 2008, pp. 33–38.

[56] C. Funk, P. Peterson, M. Landsfeld, D. Pedreros, J. Verdin, S. Shukla, G. Husak, J. Rowland, L. Harrison, A. Hoell, J. Michaelsen, The climate hazards infrared precipitation with stations - a new environmental record for monitoring extremes, Sci. Data 2 (2015) 1–21, https://doi.org/10.1038/sdata.2015.66.

[57] D.J. Westberg, P.W. Stackhouse, D.B. Crawley, J.M. Hoell, W.S. Chandler, T. Zhang, An analysis of NASA's merra meteorological data to supplement observational data for calculation of climatic design conditions, Build. Eng. 119 (2013) 210–221.

[58] S.M. Vicente-Serrano, S. Beguería, J.I. Lo´pez-Moreno, A multiscalar drought index sensitive to global warming: the standardized precipitation evapotranspiration index, J. Clim. 23 (2010) 1696–1718, https://doi.org/10.1175/2009JCLI2909.1.

[59] S.K. McFeeters, The use of the Normalized Difference Water Index (NDWI) in the delineation of open water features, Int. J. Rem. Sens. 17 (1996) 1425–1432, https://doi.org/10.1080/01431169608948714.

[60] L. Ji, L. Zhang, B. Wylie, Analysis of Dynamic Thresholds for the Normalized Difference Water Index, vol. 75, 2009, pp. 1307–1317.

[61] E. O¨zelkan, Water body detection analysis using NDWI indices derived from landsat-8 OLI, Pol. J. Environ. Stud. 29 (2020) 1759–1769, https://doi.org/10.15244/pjoes/110447.

[62] R. Makwinja, Y. Inagaki, S.G. Tesfamichael, C.J. Curtis, Novel methods for monitoring low chlorophyll-a concentrations in the large, oligotrophic Lake Malawi/Nyasa/Niassa, J. Environ. Manag. 364 (2024) 121462, https://doi.org/10.1016/j.jenvman.2024.121462.

[63] FAO/UNESCO, The digital soil map of the worldFood Agric. Organ. United Nations version 3.6, 2003 completed January.

[64] Z.A. Tilahun, Y.K. Bizuneh, A.G. Mekonnen, A spatio-temporal analysis of the magnitude and trend of land use/land cover changes in Gilgel Gibe Catchment, Southwest Ethiopia, Heliyon 10 (2024) e24416, https://doi.org/10.1016/j.heliyon.2024.e24416.

[65] A. Ahmed, B. Rotich, K. Czimber, Assessment of the environmental impacts of conflict-driven Internally Displaced Persons: a sentinel-2 satellite based analysis of land use/cover changes in the Kas locality, Darfur, Sudan, PLoS One 19 (2024) 1–19, https://doi.org/10.1371/journal.pone.0304034.

[66] N. Karasiak, Museo ToolBox: a Python library for remote sensing including a new way to handle rasters, J. Open Source Softw. 5 (2020) 1978, https://doi.org/10.21105/joss.01978.

[67] F. Pedregosa, G. Varoquaux, A. Gramfort, V. Michel, B. Thirion, Scikit-learn: machine learning in Python, J. OfMachine Learn. Res. 12 (2011) 2825–2830, https://doi.org/10.1289/EHP4713.

[68] V.F. Rodriguez-Galiano, B. Ghimire, J. Rogan, M. Chica-Olmo, J.P. Rigol-Sanchez, An assessment of the effectiveness of a random forest classifier for land-cover classification, ISPRS J. Photogrammetry Remote Sens. 67 (2012) 93–104, https://doi.org/10.1016/j.isprsjprs.2011.11.002.

[69] F. Thonfeld, S. Steinbach, J. Muro, F. Kirimi, Long-term land use/land cover change assessment of the Kilombero catchment in Tanzania using random forest classification and robust change vector analysis, Rem. Sens. 12 (2020), https://doi.org/10.3390/rs12071057.

[70] R.G. Congalton, K. Green, Assessing the Accuracy of Remotely Sensed Data Principles and Practices, Third Edition, 2019.

[71] K. Borhara, B. Pokharel, B. Bean, L. Deng, S.S. Wang, On Tanzania's precipitation climatology, variability, and future projection, Climate 8 (2020) 2–18.

[72] F. Polong, H. Chen, S. Sun, V. Ongoma, Temporal and spatial evolution of the standard precipitation evapotranspiration index (SPEI) in the Tana River Basin, Kenya, Theor. Appl. Climatol. 138 (2019) 777–792, https://doi.org/10.1007/s00704-019-02858-0.

[73] M.F.W. Slegers, "If only it would rain": farmers' perceptions of rainfall and drought in semi-arid central Tanzania, J. Arid Environ. 72 (2008) 2106–2123, https://doi.org/10.1016/j.jaridenv.2008.06.011.

[74] A.L. Kijazi, C.J.C. Reason, Analysis of the 1998 to 2005 drought over the northeastern highlands of Tanzania, Clim. Res. 38 (2009) 209–223, https://doi.org/10.3354/cr00784.

[75] C.M. Leweri, M.J. Msuha, A.C. Treydte, Rainfall variability and socio-economic constraints on livestock production in the Ngorongoro Conservation Area, Tanzania, SN Appl. Sci. 3 (2021) 1–10, https://doi.org/10.1007/s42452-020-04111-0.

[76] M.V. Mdemu, Community's vulnerability to drought-driven water scarcity and food insecurity in central and northern semi-arid areas of Tanzania, Front. Clim. 3 (2021) 1–14, https://doi.org/10.3389/fclim.2021.737655.

[77] S.L. Verhoeve, T. Keijzer, R. Kaitila, J. Wickama, G. Sterk, Northern Tanzania, Rem. Sens. 13 (2021) 4592, https://doi.org/10.1007/978-94-011-7129-8_15.

[78] G. Gebremeskel, Q. Tang, S. Sun, Z. Huang, X. Zhang, X. Liu, Droughts in East Africa: causes, impacts and resilience, Earth Sci. Rev. 193 (2019) 146–161, https://doi.org/10.1016/j.earscirev.2019.04.015.

[79] L. Janssens de Bisthoven, M.P.M. Vanhove, A.J. Rochette, J. Huge´, S. Verbesselt, R. Machunda, L. Munishi, M. Wynants, A. Steensels, M. Malan-Meerkotter, S. Henok, T. Nhiwatiwa, B. Casier, Y.A. Kiwango, R. Kaitila, H. Komakech, L. Brendonck, Social-ecological assessment of Lake Manyara basin, Tanzania: a mixed method approach, J. Environ. Manag. 267 (2020), https://doi.org/10.1016/j.jenvman.2020.110594.

[80] R. Makwinja, Y. Inagaki, T. Sagawa, J.P. Obubu, E. Habineza, W. Haaziyu, Monitoring trophic status using in situ data and Sentinel-2 MSI algorithm: lesson from Lake Malombe, Malawi, Environ. Sci. Pollut. Res. 30 (2023) 29755–29772, https://doi.org/10.1007/s11356-022-24288-8.

[81] H. Lyu, T. Watanabe, M. Kilasara, S. Funakawa, Effects of climate on distribution of soil secondary minerals in volcanic regions of Tanzania, Catena 166 (2018) 209–219, https://doi.org/10.1016/j.catena.2018.04.005.

[82] A.M. Domínguez-rodrigo, F. Díez-martín, A. Mabulla, L. Luque, L. Alcala´, A. Tarrin˜o, J.A. Lo´pez-s´aez, R. Barba, P. Bushozi, M. Domínguez-rodrigo, F. Díez-martín, A. Mabulla, L. Luque, L. Alcala´, A. Tarrin˜o, J.A. Lo´pez-sa´ez, R. Barba, P. Bushozi, The archaeology of the middle pleistocene deposits of Lake Eyasi, Tanzania, J. African Archaeol. 5 (2007) 47–78, https://doi.org/10.3213/1612-1651-10085.

[83] T.J. Pierre, N.J. Pierre, B.M. Achile, B.S. Djakba, B.D. Lucien, Morphological , Physico Chemical , Mineralogical and Geochemical Properties of Vertisols Used in Bricks Production in the Logone Valley (Cameroon , Central Africa), vol. 5, 2015, pp. 20–30.

[84] M. Orzechowski, S. Smo´lczyn´ski, B. Kalisz, Physical , Water and Redox Properties of Vertisols of the S Ę Popol Plain in North-Eastern Poland, vol. 71, 2020, pp. 185–193.

[85] S.K. Singh, P. Chandran, Soil Genesis and Classification, Soil Sci. an Introd., 2017.

[86] V. S˘imanský, Can soil properties of Fluvisols be influenced by river flow gradient, Acta Fytotech. Zootech. 2018 (2018) 63–76.

[87] G.A. Asongwe, B.P.K. Yerima, A.S. Tening, I.B. Bame, Pedogenic and contemporary issues of fluvisol characterization and utilisation in the wetlands of bamenda municipality, Cameroon, Asian Soil Res. J. 4 (2020) 8–27, https://doi.org/10.9734/ASRJ/2020/v4i330093.

[88] ISRIC, Major soil group of the world, Int. Soil Ref. Inf. Cent. (2014) 1–8.

[89] ISRIC, ANDOSOLS (AN) Summary Description of Andosols, 2016.

[90] U. Ring, D. Livingstone, H.M. Stanley, G. Fischer, The East African Rift system, Austrian J, Earth Sci. 107/1 (2014) 132–146.

[91] M.G. Sisay, E.A. Tsegaye, A.R. Tolossa, J. Nyssen, A. Frankl, E. Van Ranst, S. Dondeyne, Soil-forming factors of high-elevation mountains along the East African Rift Valley: the case of the mount guna volcano, Ethiopia, Soil Syst 8 (2024) 38, https://doi.org/10.3390/soilsystems8020038.

[92] P. Schad, The International Soil Classification System WRB, Third Edition, 2014, 2016, https://doi.org/10.1007/978-3-319-24409-9_25.

[93] P. Schad, World reference base for soil resources—its fourth edition and its history, J. Plant Nutr. Soil Sci. 186 (2023) 151–163, https://doi.org/10.1002/jpln.202200417.

[94] F. Roozitalab, H. M, N. Toomanian, V.R. Ghasemi Dehkordi, Khormali, Major soils, properties, and classification, in: Soils Iran, 2018, pp. 93–147.

[95] A.E. Ringwood, S.E. Kesson, W. Hibberson, N. Ware, Origin of kimberlites and related magmas, Earth Planet Sci. Lett. 113 (1992) 521–538, https://doi.org/10.1016/0012-821X(92)90129-J.

[96] R.S.J. Sparks, R.A. Brooker, M. Field, J. Kavanagh, J.C. Schumacher, M.J. Walter, J. White, The nature of erupting kimberlite melts, Lithos 112 (2009) 429–438, https://doi.org/10.1016/j.lithos.2009.05.032.
[97] V.S. Kamenetsky, A.V. Golovin, R. Maas, A. Giuliani, M.B. Kamenetsky, Y. Weiss, Towards a new model for kimberlite petrogenesis: evidence from unaltered kimberlites and mantle minerals, Earth Sci. Rev. 139 (2014) 145–167, https://doi.org/10.1016/j.earscirev.2014.09.004.
[98] A. Giuliani, A. Soltys, D. Phillips, V.S. Kamenetsky, R. Maas, K. Goemann, J.D. Woodhead, R.N. Drysdale, W.L. Griffin, The final stages of kimberlite petrogenesis: petrography, mineral chemistry, melt inclusions and Sr-C-O isotope geochemistry of the Bultfontein kimberlite (Kimberley, South Africa), Chem. Geol. 455 (2017) 342–356, https://doi.org/10.1016/j.chemgeo.2016.10.011.
[99] V.S. Kamenetsky, E.A. Belousova, A. Giuliani, M.B. Kamenetsky, K. Goemann, W.L. Griffin, Chemical abrasion of zircon and ilmenite megacrysts in the Monastery kimberlite: implications for the composition of kimberlite melts, Chem. Geol. 383 (2014) 76–85, https://doi.org/10.1016/j.chemgeo.2014.06.008.
[100] S. Tetiker, H. Yalçın, O¨. Bozkaya, Evidence of the diagenetic history of sediment composition in precambrian-early paleozoic rocks: a systematic study from the southeast anatolian autochthon, mardin (Derik-Kızıltepe), Turkey, Arabian J. Geosci. 8 (2015) 11261–11278, https://doi.org/10.1007/s12517-015-2006-1.
[101] V.G. Kuznetsov, Geochemical environments of precambrian sedimentation, Lithol. Miner. Resour. 55 (2020) 99–110, https://doi.org/10.1134/S0024490220010034.
[102] E.S.A. Saber, Gold resources from clastic Cambrian rocks and their link with underlying Precambrian rocks, southern Sinai, Egypt, Arabian J. Geosci. 13 (2020), https://doi.org/10.1007/s12517-020-05526-0.
[103] J.R. Landis, G.G. Koch, The measurement of observer agreement for categorical data data for categorical of observer agreement the measurement, Biometrics 33 (1977) 159–174, https://doi.org/10.2307/2529310.
[104] S.M. Onywere, Use of remote sensing data in evaluating the extent of anthropogenic activities and their impact on lake Naivasha, Kenya, Open Environ. Eng. J. 5 (2012) 9–18, https://doi.org/10.2174/1874829501205010009.
[105] S. Chaudhari, F. Felfelani, S. Shin, Y. Pokhrel, Climate and anthropogenic contributions to the desiccation of the second largest saline lake in the twentieth century, J. Hydrol. 560 (2018) 342–353, https://doi.org/10.1016/j.jhydrol.2018.03.034.
[106] N.B. Of S.T. Ministry of Finance and Planning, Age and Sex Distribution Report, 2022, pp. 1–23.
[107] J. Onyango, K. Irvine, J.J.A. Van Bruggen, N. Kitaka, N. Kreuzinger, Agricultural expansion and water pollution : the yin-yang in the quality of natural water resources, african cent, Technol. Stud. 9 (2015) 1–29.
[108] A.E. Evans, J. Mateo-Sagasta, M. Qadir, E. Boelee, A. Ippolito, Agricultural water pollution: key knowledge gaps and research needs, Curr. Opin. Environ. Sustain. 36 (2019) 20–27, https://doi.org/10.1016/j.cosust.2018.10.003.
[109] D.W. Goshime, R. Absi, B. Lede´sert, F. Dufour, A.T. Haile, Impact of water abstraction on the water level of Lake Ziway, Ethiopia, WIT Trans. Ecol. Environ. 239 (2019) 67–78, https://doi.org/10.2495/WS190071.
[110] F. Yao, B. Livneh, B. Rajagopalan, J. Wang, J.F. Cr´etaux, Y. Wada, M. Berge-Nguyen, Satellites reveal widespread decline in global lake water storage, Science 380 (2023) 743–749, https://doi.org/10.1126/SCIENCE.ABO2812.
[111] P.Z. Yanda, N.F. Madulu, Water resource management and biodiversity conservation in the Eastern Rift Valley lakes, northern Tanzania, Phys. Chem. Earth 30 (2005) 717–725, https://doi.org/10.1016/j.pce.2005.08.013.